be that the ligand deficient samarium centers readily form 2:1 $(C_5Me_5)_2Sm$:(unsaturated substrate) complexes. The tetracyclopentadienyl cavity generated in this way may provide an environment in which reactions not possible in bulk solution can occur. The formation of dynamic tetracyclopentadienyl cavities of this type may be available in other systems and should be pursued as a means of accomplishing rapid, quantitative cage chemistry without constructing a rigid enclosure.

Acknowledgment. We thank the National Science Foundation for support of this research. Funds for the purchase of the Nicolet R3m/V diffractometer system were made available from the National Science Foundation under Grant CHE-85-14495.

Supplementary Material Available: Tables of crystal data, final fractional coordinates, hydrogen atom coordinates, bond distances and angles, and thermal parameters (45 pages); tables of observed and calculated structure factors (74 pages). Ordering information is given on any current masthead page.

Molecular Hydrogen Complexes. 6. The Barrier to Rotation of η^2-H_2 in $M(CO)_3(PR_3)_2(\eta^2$-$H_2)$ (M = W, Mo; R = Cy, *i*-Pr): Inelastic Neutron Scattering, Theoretical, and Molecular Mechanics Studies

Juergen Eckert,*,† Gregory J. Kubas,*,‡ John H. Hall,‡ P. Jeffrey Hay,*,§ and Caroline M. Boyle§

Contribution from the Los Alamos Neutron Scattering Center, MS H805, Inorganic and Structural Chemistry Group (INC-4), MS-C346, and Theoretical Chemistry and Molecular Physics Group (T-12), MS-J569, Los Alamos National Laboratory, Los Alamos, New Mexico, 87545, and Institut Laue-Langevin, 156X, 38042 Grenoble Cedex, France.
Received July 31, 1989

Abstract: Inelastic neutron scattering (INS) studies, electronic structure calculations, and molecular mechanics have been carried out on a series of molecular hydrogen complexes, $M(CO)_3(\eta^2$-$H_2)(PR_3)_2$ (M = Mo, W, R = c-C_6D_{11}; M = W, R = *i*-C_3D_7), in order to determine relative electronic versus steric (ligand bulk) effects on the barrier to rotation of the H_2 ligand. Low-lying vibrational excitations were identified with INS, and high-resolution spectrometers were used to measure the rotational tunneling splitting of the librational ground state on the solid complexes at 4 K. Replacement of the W by Mo changed the latter splitting by about a factor of 3, from 0.89 to 2.82 cm^{-1}. Variation of the phosphine on the other hand changed the frequency by less than 20%. The torsional transitions observed in the range 300–400 cm^{-1} are consistent with the tunneling transitions for a simple double-minimum potential with one angular degree of freedom for the rotation. The barrier heights hindering the H_2 rotation were determined from these measurements to be 2.4 kcal/mol (M = W, R = *i*-Pr), 2.2 kcal/mol (M = W, R = Cy), and 1.5–1.7 kcal/mol (M = Mo, R = Cy). Ab initio electronic structure calculations showed that the electronic component yields barriers of 1.4–1.8 kcal/mol for M = W and R = H, of 0.8 kcal/mol for M = W and R = Me, and of 0.6 kcal/mol for M = Mo and R = H. The present calculations show the simple double-minimum potential with the minima parallel to the P–M–P axis, which is indeed observed to be the equilibrium position for the H_2 in the crystallographic studies. Molecular mechanics (MM2) calculations showed no direct steric effects arising from the bulky phosphine ligands on the H_2 rotational barrier but did show an additional orientational preference (0.6–1.4 kcal/mol) for the H_2 along the P–M–P axis. The sum of the calculated ab initio and MM2 barriers agreed remarkably well with the observed INS values.

The nature of bonding of the dihydrogen ligand to transition metals is of major significance because $M(\eta^2$-$H_2)$ represents the prototype for ligand coordination solely via interaction of a metal center with a σ-bonding electron pair ("σ-bond complex").[1,2] This three-center, two-electron bonding is electron-deficient similar to boron hydrides and serves as a model for as yet unisolated alkane complexes (C–H coordination). Theoretical studies[3] indicate that the primary interaction is donation of electron density from the H–H σ bond to an empty metal orbital and that a lesser degree of metal to H_2 σ^* back-bonding analogous to metal to olefin π^* back-donation also occurs. The latter stabilizes the side-on (η^2) coordination mode and ultimately facilitates cleavage of the H–H bond to give dihydride complexes in oxidative addition reactions (Chart I). An experimental probe of the electronic details of dihydrogen coordination is clearly desirable. η^2-H_2 undergoes a remarkably wide variety of ligand dynamics, including rapid

Chart I

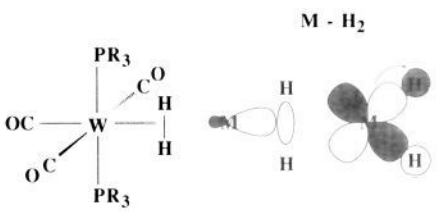

rotation about the M–H_2 axis.[1] The presence and magnitude of an energy barrier to rotation that is electronic in origin would offer

† Los Alamos Neutron Scattering Center and Institut Laue-Langevin. Send correspondence to Los Alamos National Laboratory.

‡ Inorganic and Structural Chemistry Group, Los Alamos National Laboratory.

§ Theoretical Chemistry and Molecular Physics Group, Los Alamos National Laboratory.

(1) (a) Kubas, G. J. *Acc. Chem. Res.* **1988**, *21*, 120. (b) Kubas, G. J.; Unkefer, C. J.; Swanson, B. I.; Fukushima, E. *J. Am. Chem. Soc.* **1986**, *108*, 7000.

(2) Crabtree, R. H.; Hamilton, D. G. *Adv. Organomet. Chem.* **1988**, *28*, 299.

(3) (a) Bagatur'yants, A. A.; Anikin, N. A.; Zhidomirov, G. M.; Kazanskii, V. B. *Zh. Fiz. Khim.* **1981**, *55*, 2035. (b) Hay, P. J. *Chem. Phys. Lett.* **1984**, *103*, 466. (c) Saillard, J.-Y.; Hoffmann, R. *J. Am. Chem. Soc.* **1984**, *106*, 2006. (d) Hay, P. J. *J. Am. Chem. Soc.* **1987**, *109*, 705. (e) Jean, Y.; Eisenstein, O.; Volatron, F.; Maouche, B.; Sefta, F. *J. Am. Chem. Soc.* **1986**, *108*, 6587. (f) Jean, Y.; Lledos, A. *Nouv. J. Chim.* **1987**, *11*, 635. (g) Jean, Y.; Lledos, A.; Maouche, B.; Alad, R. *J. Chim. Phys.* **1987**, *84*, 805.

0002-7863/90/1512-2324$02.50/0

confirmation of M → H_2 back-donation. The barrier is too small to be observed by standard NMR methods, but inelastic neutron scattering (INS) methods have been routinely employed to study rapid rotational motion (e.g., Me groups, H_2).[4,5] We have now utilized INS to investigate the dynamics of the first complexes discovered[1,6] to contain a dihydrogen ligand, $M(CO)_3(PR_3)_2(H_2)$ (M = Mo, W; R = cyclohexyl (Cy), *i*-Pr), and to obtain experimental values for the barrier to rotation of the H_2.

We recently reported a direct observation by INS of the rotational tunneling of η^2-H_2 at low temperature in $W(CO)_3(PCy_3)_2(H_2)$.[5] These rotational tunneling transitions (essentially para (I = 0, J = 0) to ortho (I = 1, J = 1) transitions within the ground librational state of the H_2 molecule) were found to persist up to nearly 190 K, which well may be the highest temperature at which this quantum mechanical process has been observed. The size of the tunnel splitting of the bound dihydrogen in $W(CO)_3(\eta^2\text{-}H_2)[P(c\text{-}C_6D_{11})_3]_2$ was found to be 0.95 (1) cm^{-1}, and in addition, H_2 torsions (i.e., transitions to excited librational states) were observed at 325 and 380 cm^{-1}. These data can be well accounted for by a model[5,7] of reorientation of the dihydrogen in a plane perpendicular to the OC–W–H_2 axis in a double-minimum potential. The rotational barrier height V_2 derived from this analysis was 760 cm^{-1}, or 2.18 kcal/mol (assuming an H–H bond length of 0.82 Å as found[6,8] for $W(CO)_3(P\text{-}i\text{-}Pr_3)_2(H_2)$). An important question is to what degree this barrier is determined by the binding of H_2 to the metal (electronic effects) relative to possible steric effects of the bulky phosphines.

One may attempt to decide this question by comparison with theoretical calculations of this problem. Ab initio electronic structure calculations by Hay[3d] on $W(CO)_3(PH_3)_2(H_2)$ correctly predicted the actual equilibrium orientation (H–H axis parallel to P–W–P) but yielded an energy difference between this orientation and the one perpendicular to it (H–H parallel to OC–W–CO) of only 0.3 kcal/mol. Since this calculation drastically overestimated the W–H distances (2.15 vs 1.89 Å actually found in $W(CO)_3(P\text{-}i\text{-}Pr_3)_2(H_2)$), it seems reasonable, therefore, that the actual barrier to H_2 rotation might be significantly higher than this value. Jean et al.[3e-g] using extended Hückel methods calculated the energy of a $WH_2(CO)_3(\eta^2\text{-}H_2)$ model complex as a function of W–H_2 separation for both parallel and perpendicular orientations. Their value of the energy difference between the two orientations of 2.1 kcal/mol was determined with an assumed W–H_2 distance of 1.7 Å, which is somewhat too short. In either case, the energy difference between the orientations may only represent a lower limit of the total barrier to rotation since the possible steric effects arising from the bulky phosphine ligands are not incorporated into such calculations. Thus, while one may conclude from the prior theoretical results that a significant portion of the barrier stems from the electronic interaction of H_2 with the metal, further experimental studies are required to answer this question.

We have therefore carried out a series of experiments in which either the metal (Mo, W) or the phosphine (PCy_3, P-*i*-Pr_3; cone angles[9] 170° and 160°, respectively) was changed, and the barrier to H_2 rotation was determined from the rotational ground-state tunnel splitting by previously reported methods.[5,10] In addition, molecular mechanics calculations, ab initio calculations with improved metal–dihydrogen geometry, and Fenske–Hall calculations have been carried out to assist in interpretation of the rotational barrier results obtained from the neutron scattering experiments.

Experimental Section

Synthesis of $M(CO)_3(PR_3)_2(H_2)$ with Perdeuteriophosphines. The preparations with inert atmosphere procedures are similar to those previously reported.[1b] The phosphines $P(c\text{-}C_6D_{11})_3$ and $P(i\text{-}C_3D_7)_3$ (ca. 98 atom % D) were obtained on a custom synthesis basis from MSD Isotopes, Montreal, Canada, as their CS_2 adducts. In order to prepare pure H_2 complexes, it was necessary to scrupulously remove all traces of CS_2 by heating the adducts in alcohols and driving off the CS_2 by distillation until the solutions became completely colorless. For R = C_6D_{11}, ethanol (~15 mL per g of $PR_3 \cdot CS_2$) was used and the solid phosphine was isolated by removing the remaining ethanol in vacuo.

For R = C_3D_7, some phosphine distilled over along with CS_2 when ethanol was used, so the procedure was modified by heating the adduct (2.4 g) in methanol (10 mL) in a 15-mL flask and distilling off MeOH–CS_2 at a slower rate. Most of the methanol was removed by distillation, and the remainder was carefully pumped off in vacuo at 0 °C, with a final pumping at 25 °C for 5 min only (the liquid phosphine is slightly volatile). The $P(C_3D_7)_3$ (yield: ~1.7 mL, ~1.4 g) was then syringed into another 15-mL flask to separate it from insoluble matter. The original flask was washed with 3 mL of hexane, which was added to the second flask, and the resulting mixture was then reacted with $W(CO)_3$(cycloheptatriene) (1.4 g) under H_2 to give $W(CO)_3[P(C_3D_7)]_2(H_2)$ (1.13 g).

Inelastic Neutron Scattering. The inelastic neutron scattering experiments used to determine rotational tunneling modes were carried out on the high-resolution time-of-flight spectrometer IN5 at the high-flux reactor of the Institut Laue-Langevin in Grenoble, France. The energy resolution and energy transfer range of this instrument depend on the incident energy (or wavelength) selected for a given run. Because of the relatively wide range of rotational tunnel splittings observed in this study, wavelengths of 6, 8, or 10 Å were used for the different samples in this study. Approximately 2 g of complex (containing perdeuteriophosphines to lower background scattering) was sealed in aluminum containers under H_2-enriched argon atmospheres. Counting times for this amount of material ranged from 10 to 18 h, depending on the incident neutron wavelength.

Additional experiments with similar sample containers were carried out at the Los Alamos Neutron Scattering Center to determine the torsional modes of the H_2 molecule. In order to be able to distinguish the modes of the metal–dihydrogen fragment from all the other vibrational modes in these molecules, a sample difference technique had to be employed.[11] This technique is based on the fact that the incoherent neutron scattering cross-section for hydrogen is more than 1 order of magnitude greater than that of deuterium. Vibrational modes involving deuterium are therefore relatively difficult to observe in the presence of many hydrogen atoms by inelastic neutron scattering. A subtraction of two experimental INS spectra, that of the M–(D_2) analogue from that of the M–(H_2) compound, should leave, therefore, only those peaks involving motion of the dihydrogen, provided any possible coupling of those modes to other vibrations are negligible on the scale of the resolution of the INS experiment. It was unnecessary for the samples here to contain deuterated phosphine ligands. However, the experiment requires a spectrometer with very high count rates (and therefore modest energy resolution) in order to obtain reasonable statistics on the difference data set. The filter difference spectrometer[12] at Los Alamos is well suited for this type of work on account of its very large detected solid-angle and relaxed-energy resolution. It can cover an energy range from 250 to 4000 cm^{-1} with a resolution of 2–10% of the incident neutron energy.

Molecular Mechanics Calculations. Molecular mechanics (MM2) calculations were carried out with CHEM-X[13] software running on an Evans and Sutherland PS340 graphics workstation with a Digital Equipment Corp. Vax 11/785 (VMS Version 4.7 operating system) serving as the host processor. Coordinate positions for all atoms were taken from the respective crystal structures.[6,8,14] In the case of $W(CO)_3(P\text{-}i\text{-}Pr_3)_2(H_2)$, one triisopropylphosphine ligand was disordered and was replaced by an idealized group. After conversion to orthonormal coordinates, the metal atom was set at the origin and a dummy atom was placed at the midpoint between the dihydrogen molecule atoms. The molecule was then rotated to place this dummy atom along the z axis. The MM2 energy[15] was calculated with all bond lengths, bond angles,

(4) (a) See for example: Howard, J.; Waddington, T. C. *Advances in Infrared and Raman Spectroscopy*; Clark, R. J. H., Hester, R. E., Eds.; Heyden: London, 1980; Chapter 3, Vol. 7. (b) See, for example: Press, W. *Single-Particle Rotations in Solids*; Springer Tracts in Modern Physics; Springer: Berlin, 1981; Vol. 92.

(5) Eckert, J.; Kubas, G. J.; Dianoux, A. J. *J. Chem. Phys.* **1988**, *88*, 466.

(6) Kubas, G. J.; Ryan, R. R.; Swanson, B. I.; Vergamini, P. J.; Wasserman, H. J. *J. Am. Chem. Soc.* **1984**, *106*, 451.

(7) Pauling, L. *Phys. Rev.* **1930**, *36*, 430.

(8) Vergamini, P. J.; Wasserman, H. J.; Kubas, G. J.; Koetzle, T. J.; Ryan, R. R., unpublished results.

(9) Tolman, C. A. *Chem. Rev.* **1977**, *77*, 313.

(10) Nicol, J. M.; Eckert, J.; Howard, J. *J. Phys. Chem.* **1988**, *92*, 7117.

(11) Eckert, J. *Physica* **1986**, *136B*, 150.

(12) Taylor, A. D.; Wood, E. J.; Goldstone, J. A.; Eckert, J. *Nucl. Instrum. Methods* **1984**, *221*, 408.

(13) CHEM-X is developed and distributed by Chemical Design Ltd., Oxford, England.

(14) Kubat-Martin, K. A.; Kubas, G. J.; Khalsa, G. R. K.; Van Der Sluys, L. S.; Wasserman, H. J.; Ryan, R. R. *Acta Crystallogr., Sect. C: Cryst. Struct. Commun.*, in press.

(15) Burkert, U.; Allinger, N. L. *Molecular Mechanics*; ACS Monograph 177; American Chemical Society: Washington, DC, 1982.

and torsion angles held constant and all atomic charges set to zero, leaving only Lennard-Jones nonbonding potentials with a possibility of changing. This calculation was repeated for 36 different 5° clockwise rotations of the dihydrogen molecule about the z axis. Since the atom–atom distance between the metal and the dihydrogen molecule remained constant throughout the calculation, the relative change in energy at each angle represents the rotation barrier due to steric effects for the dihydrogen molecule.

An additional set of calculations was carried out in which the isopropyl groups were removed (phosphorus atoms retained).

Ab Initio and Fenske–Hall Calculations. Ab initio electronic structure calculations were carried out on $M(CO)_3(PR_3)_2(H_2)$ species, where M = W and Mo and R = H and Me, at the Hartree–Fock self-consistent field level. Relativistic effective core potentials (ECPs)[16] were used to replace the inner electrons on W and Mo, and a nonrelativistic ECP was employed on the P atoms. The M–H_2 distance, H–H distance, and H_2 orientation relative to the P–M–P axis were varied while a fixed geometry for the CO and phosphine ligands was maintained about the metal. The coordinates for the latter ligands were taken from the experimental X-ray structure for the complex with M = W and R = Cy,[14] the structural parameters for which were also virtually identical with the Mo complex. Bond lengths were as follows: M–P, 2.511 Å; M–C_{eq}, 2.012 Å; C_{eq}–O_{eq}, 1.140 Å; M–C_{ax}, 1.99 Å; C_{ax}–O_{ax}, 1.17 Å. Octahedral bond angles were assumed. Additional structural parameters were as follows: for PH_3 ligands, P–H = 1.421 Å, M–P–H = 119°; for PMe_3 ligands, P–C = 1.87 Å, C–H = 1.09 Å, M–P–C = 115.1°, P–C–H = 109.5°.

The valence 6s, 6p, and 5d orbitals and the outer 5s and 5p core orbitals of W were explicitly treated in the calculations (and similarly the 4s, 4p, 4d, 5s, and 5p orbitals for Mo) with a double-ζ (DZ) representation for the valence orbitals and a single contracted function for the outer core orbital; this resulted in a (3s3p2d) contracted Gaussian basis for the metal. A (5s1p) primitive basis contracted to (3s1p) was used on each H of the H_2 ligand. Minimum basis set (MBS) and DZ representations were employed for the ligands. For CO this consisted of the STO-3G[17] basis at the MBS level and the (9s5p) Huzinaga basis set contracted according to Dunning and Hay[18] to (3s2p). For PMe_3, the previous MBS basis for P was used and STO-3G basis sets were used for C and H.

Nonempirical Fenske–Hall (FHT)[19] calculations were carried out for the series of complexes, M = Mo and W and R = H, Me, i-Pr, and Cy, with the actual X-ray structure[6,8,14] coordinates for the latter two ligands and idealized structures for the former two ligands to compare to the ab initio calculations. The FHT Slater-type atomic basis sets were determined with an Xα-optimized atomic basis set.[20] The atomic Xα calculations were preformed with the computer program of Herman and Skillman.[21] The α values were taken from the compilations of Schwarz, chosen so that the Xα total energy is equal to the Hartree–Fock total energy.[22] DZ representations were used for the W 5d, P 3p, C 2p, and O 2p orbitals. An exponent of 1.16 was used for the H 1s orbital.[23] The W 6s and 6p exponents were fixed at 1.8.

Experimental Results

Inelastic Neutron Scattering (INS) Spectra and Model for H_2 Rotation. INS vibrational data in the 200–1000-cm^{-1} region were collected on the filter difference spectrometer at the Los Alamos Neutron Scattering Center for both $W(CO)_3(PR_3)_2(H_2)$ and $W(CO)_3(PR_3)_2(D_2)$ (R = Cy, i-Pr). The INS spectrum of the D_2 complex was then subtracted from that of the H_2 complex, a procedure that leaves essentially only those vibrational modes involving the H_2 ligand because (a) ancillary ligand modes are canceled out and (b) the scattering intensity from the D_2 is much lower than from the H_2. While the counting statistics on these data sets are relatively poor on account of the subtraction of two large numbers, the observed features in the resultant difference

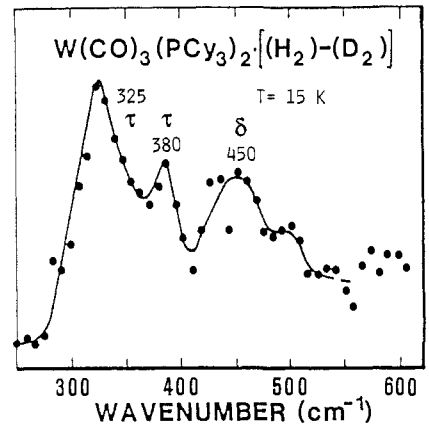

Figure 1. Vibrational INS spectrum of $W(CO)_3(P\text{-}i\text{-}Pr_3)_2[(H_2)-(D_2)]$ taken on the filter difference spectrometer.

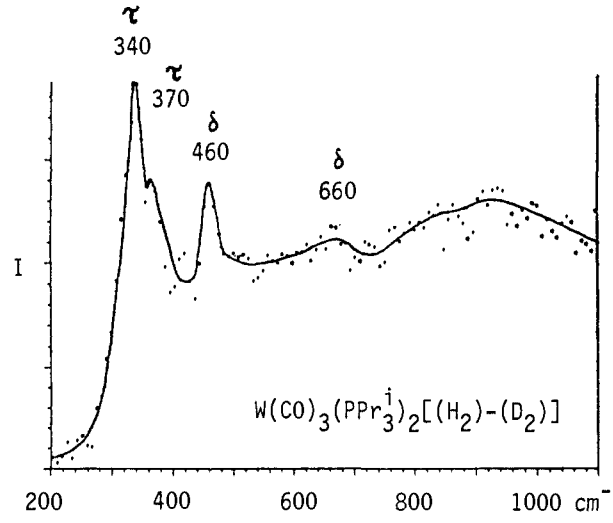

Figure 2. Vibrational INS spectrum of $W(CO)_3(PCy_3)_2[(H_2)-(D_2)]$ taken on the filter difference spectrometer.

spectra for R = i-Pr are similar to those for R = Cy, as might be expected if the effect of changing the phosphine ligand on the vibrational spectrum of the W–(H_2) fragment is relatively small. This observation gives some confidence that the subtraction procedure used to isolate the W–(H_2) vibrations is in fact reasonably valid.

The INS difference spectra of $W(CO)_3(PR_3)_2(H_2)$ are shown in Figures 1 (R = i-Pr) and 2 (R = Cy) and contain a pair of peaks between 300 and 400 cm^{-1}, a peak at about 450–460 cm^{-1}, and other, less discernible features. Previous spectroscopic studies with IR and Raman techniques[1,6,24] were able to assign four of the six vibrational modes expected for the W–(η^2-H_2) fragment: the H–H stretch (2690 cm^{-1}), the symmetric and asymmetric W–(H_2) stretches (~1570, 953 cm^{-1}), and one of the two W–(H_2) deformation (δ) modes (464 cm^{-1}). The higher energy, stretching modes are not observed in the INS, but the latter deformation agrees well with the INS data. A second deformation, not directly observed by IR or Raman for the H_2 isotopomer, is believed to occur at about 610–640 cm^{-1} on the basis of the calculated isotopic shifts of the observed mode for the D_2 analogue.[1b,24] The spectrum shown in Figure 1 shows a weak, broad feature near 660 cm^{-1} that may correspond to this deformation. As far as the assignment of the doublet in the 300–400-cm^{-1} range is concerned, it should be noted that in INS spectroscopy those modes involving large-amplitude motions of hydrogen have the highest intensity.[4a] Thus, the most probable assignment for the two peaks below 400 cm^{-1} is a split W–(H_2) torsion, which would, in general, be difficult to observe by IR or Raman techniques. It should also be noted

(16) Hay, P. J.; Wadt, W. R. *J. Chem. Phys.* **1985**, *82*, 270 and 284.
(17) Hehre, W. J.; Ditchfield, R.; Pople, J. A. *J. Chem. Phys.* **1972**, *56*, 2257.
(18) Huzinaga, S. *J. Chem. Phys.* **1965**, *42*, 1293. Dunning, T. H., Jr.; Hay, P. J. *Methods of Electronic Structure Theory*; Schaefer, H. F., III, Ed.; Plenum Press: New York, 1977; pp 1–27.
(19) Hall, M. B.; Fenske, R. F. *Inorg. Chem.* **1972**, *11*, 768.
(20) Bursten, B. E.; Jensen, J. R.; Fenske, R. F. *J. Chem. Phys.* **1978**, *68*, 3320.
(21) Herman, F.; Skillman, J. *Atomic Structure Calculations*; Prentice-Hall: Englewood Cliffs, NJ, 1983.
(22) (a) Schwarz, K. *Phys. Rev.* **1972**, *B5*, 3321. (b) Schwarz, K. *Theor. Chim. Acta* **1974**, *34*, 225.
(23) Hehre, W. J.; Stewart, F. F.; Pople, J. A. *J. Chem. Phys.* **1969**, *51*, 2657.
(24) Swanson, B. I.; Kubas, G. J.; Eckert, J.; Jones, L. Unpublished results.

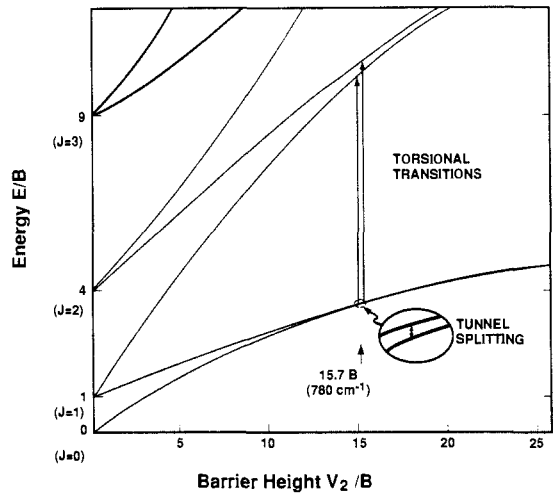

Figure 3. Energy levels of hindered H_2 rotation in a double-minimum potential. The observed transitions for H_2 coordinated to tungsten are indicated by arrows. Energy levels and potential barriers are given in terms of the rotational constant B.

that while the stretching and deformation modes show little dependence (<5 cm^{-1} in the IR) on the alkyl substituent (Cy vs *i*-Pr), there are much greater shifts (up to 20 cm^{-1}) in the torsions.

The model we use to interpret the data on the rotational transitions and derive a value for the barrier height is one of planar rotation of the H_2 ligand with one degree of rotational freedom. The reason for this choice is that we assume that the relatively strong three-center metal–dihydrogen bond keeps the H_2 ligand essentially in a plane during its torsional and rotational tunneling motions. This may in fact be an example of hydrogen molecular rotation with only one degree of freedom as described by Pauling[7] as an approximation for solid H_2. If any mixing with vibrational modes can be neglected, the Schrödinger equation for the rotational motion is

$$[-B(\partial^2/\partial\phi^2) + \tfrac{1}{2}\sum V_{2n}(1 - \cos 2n\phi)]\Psi = E\Psi \qquad (1)$$

where ϕ is the angle of rotation about the O–C–W–H_2 axis and B is the rotational constant. Since in the present case crystal structure studies, as well as theoretical calculations, have shown the dihydrogen to have a well-defined orientation parallel to the P–W–P axis, we may assume that the term with $n = 1$, i.e., a simple double-minimum potential, will dominate. Equation 1 can then be reduced to the Mathieu equation for which the solutions are tabulated.[25] The energy level diagram as function of barrier height V_2 is shown in Figure 3, where both the energies and barriers are given in terms of B, which here is taken to be 49.5 cm^{-1} rather than 60 cm^{-1} for free H_2 on the basis of diffraction data[6,8] that show an increased H–H bond length (0.82 Å) relative to free H_2 (0.74 Å). For $V_2 = 0$ the free rotor energy levels are given by $E_J = BJ^2$ (the states for $J^2 = 0$, 1, 4, and 9 are shown in Figure 3), whereas in the limit of very high barriers we have a torsional oscillator with equally spaced energy levels. For *intermediate* barrier heights as we have here, there exists a series of split librational states, where the transition to the first excited state, for example, is also referred to as the torsion. The transition within the ground librational state corresponds to the para ($I = 0$, $J = 0$) to ortho ($I = 1$, $J = 1$) transition for the hydrogen molecule, which has a value of 120 cm^{-1} in liquid hydrogen, for example. It is important to note that this value rapidly decreases as the barrier is increased (Figure 3) and that it is observable by INS (see below).

The INS bands assigned as torsions (τ) for the W–PR_3 complexes are indicated in Figures 1 and 2 and tabulated in Table I. One can obtain calculated values of the torsions by using data fitting techniques and assuming the potential $V = {}^1/_2V_2(1 - \cos$ $(2\phi))$ where V_2 (barrier height) is determined by the ground-state splitting measured by INS (rotational tunneling spectra, see below). The latter splittings of 0.89 cm^{-1} (R = Cy) and 0.73 cm^{-1} (R = *i*-Pr) corresponded to barrier heights of 15.7B or 780 cm^{-1} and 16.4B or 815 cm^{-1}, respectively. From these values of V_2, energy level diagrams such as that shown in Figure 3 were then used to predict the torsional transitions. The calculated values are in good agreement with experiment (Table I), which suggests that the simple model of planar reorientation in a double-minimum potential gives a reasonable description for the hydrogen motion in these systems. The rate of H_2 rotation is estimated to be on the order of 10^{11} s^{-1}.

Table I. Observed and Calculated Rotational Energy Levels (cm^{-1}) for $W(CO)_3(PR_3)_2(\eta^2\text{-}H_2)$ (Calculated Levels for a Potential $V = {}^1/_2V_2(1 - \cos(2\phi))$ Where V_2 Is Determined by the Ground-State Splitting)

R = Cy		R = *i*-Pr	
obsd	calcd	obsd	calcd
0.89[a]		0.73[a]	
325	328	340	340
380	350	370	360
(V_2 = 780)		(V_2 = 815)	

[a] Uses intensity-weighted mean frequencies from present work.

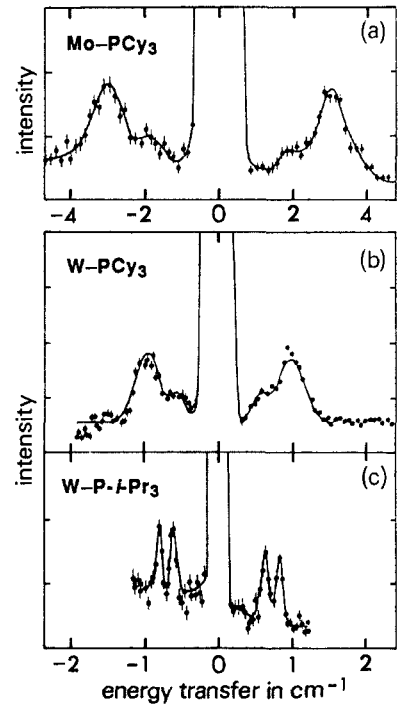

Figure 4. Rotational tunneling spectra of (a) $Mo(CO)_3[P(c\text{-}C_6D_{11})_3]_2(H_2)$, (b) $W(CO)_3[P(c\text{-}C_6D_{11})_3]_2(H_2)$, and (c) $W(CO)_3[P(i\text{-}C_3D_7)_3]_2(H_2)$ at 4 K (note different scale in (a)).

The position of the split torsional peaks, namely 325 and 380 cm^{-1} for the PCy_3 complex and 340 and 370 cm^{-1} for the P-*i*-Pr_3 complex, indicates that the barrier in the latter (815 cm^{-1}, 2.4 kcal/mol) is slightly higher than in the former (780 cm^{-1}, 2.2 kcal/mol). Also, the potential may have some components of higher than 2-fold symmetry,[4b] since agreement of experimental and calculated energy levels within this simple model is not exact.[5]

Rotational Tunneling Spectra. High-resolution INS spectra of the librational ground-state tunnel splitting were obtained on the cold-neutron time-of-flight spectrometer IN5 at the high-flux reactor of the Institut Laue-Langevin (ILL) in Grenoble. No blank samples were needed because the other ligands would not be expected to have observable excitations in the frequency range of interest (<10 cm^{-1}). However, fully deuterated phosphine ligands were used in these experiments to reduce elastic scattering background. Spectra are shown in Figure 4 for three complexes. The inelastic scattering peaks of interest are located on either side

(25) Abramowitz, M.; Segun, I. A. *Handbook of Mathematical Functions*; Dover Press: New York, 1968.

Table II. Calculated and Experimental Geometries for $M(CO)_3(PR_3)_3(H_2)$ Complexes from ab Initio Calculations

			distance (Å)			vibrational frequency (cm^{-1})	
	M	R	M-H_2	M-H	H-H	M-H_2	H-H
calcd	W	H	1.867	1.911	0.812	963	3181
exptl	W	*i*-Pr	1.845	1.89	0.82	953	2690
calcd	Mo	H	1.951	1.990	0.784	839	3834
exptl	Mo	Cy				871	2950
calcd	H_2 (free)				0.734		4523
exptl	H_2 (free)				0.741		4401

of the large elastic peak that is ~100–200 times more intense. The transitions are observed in both neutron energy gain (positive energy) and energy loss because the system will not readily relax to the lowest level, a process requiring spin conversion for the H_2 ligand. In inelastic neutron scattering, transitions within the librational levels involving a change in the total nuclear spin of the molecule ($\Delta I = \pm 1$) are allowed (in addition to $\Delta I = 0$) because the interaction between the neutron and the scatterer is with nuclei rather than electrons as in optical spectroscopy. Thus, for example, the para ($I = 0$, J even) to ortho ($I = 1$, J odd) transition for the hydrogen molecule can be observed directly by INS, as can its equivalent in the case of a hindered H_2 rotor. It should be kept in mind that a smaller tunnel splitting of the ground state indicates an *exponentially higher* barrier to rotation.

First, it must be noted that these spectra reveal doublet-type splittings that could not have been observed in the earlier low-resolution experiment.[5] The probable origin of this fine structure will become apparent below. More importantly, a comparison of the spectra shows that replacement of W (Figure 4b) with Mo (Figure 4a) changes the intensity-weighted mean tunneling frequency by about a factor of 3 from 0.89 to 2.82 cm^{-1}. Varying the phosphines on the W complex, on the other hand, from PCy_3 (Figure 4b) to P-*i*-Pr_3 (Figure 4c) changes the frequency by less than 20% from 0.89 to 0.73 cm^{-1}. It is therefore obvious that replacement of the metal center has a much greater effect on the rotational tunnel splitting (and thus the barrier to rotation) than that of the phosphine ligands used. The former may be taken to reflect the metal–dihydrogen binding directly, i.e., essentially an electronic effect. Replacement of the PCy_3 by P-*i*-Pr_3, on the other hand, has in all likelihood little effect on the electronic state of the metal and, therefore, the metal–H_2 binding. These ligands most likely produce a steric component of the barrier to H_2 rotation through direct, nonbonded atom–atom interactions. It would appear, therefore, that at least in these cases the experimental evidence strongly suggests that the barrier to H_2 rotation is determined to a greater extent by electronic than by steric effects. In order to test and substantiate this conclusion, we have carried out new ab initio and molecular mechanics calculations whose results will be discussed below in view of the present experiments.

The observed secondary structure in the rotational tunneling spectra (Figure 4), on the other hand, may most likely be attributed to structural disorder. The reason for this conclusion is that it is consistent with crystallographic information available on these systems and that other possible explanations may be ruled out. First, it should be noted that the rotational tunneling spectra of both PCy_3 complexes (Figure 4a,b) have qualitatively similar shapes, a broadened doublet with an intensity ratio of 3:1, while the spectrum of the P-*i*-Pr_3 complex (Figure 4c) has a sharp 1:1 doublet. It is also known from crystal structure studies[6,8] that in the P-*i*-Pr_3 complex one of the phosphines is disordered and has two possible orientations, each of which could give rise to a slightly different hindering potential at the site of the H_2. If the two conformations occur in the solid in a 1:1 ratio, two closely spaced peaks in 1:1 intensity ratio would be expected in the rotational tunneling spectrum, as is indeed observed (Figure 4c). The disorder in the PCy_3 complexes indicated by their rotational tunneling spectra would appear to be more complex as the peaks are significantly broadened in addition to showing unequal intensities. Crystal structure studies[14] on these compounds have in fact been unable to give a precise location of the H_2 because of positional disorder between the H_2 and the *trans*-CO ligand in the triclinic structures (space group $P\bar{1}$).

Two other possible causes for the structure in the rotational tunneling spectra can unambiguously be ruled out, namely that the symmetry of the orientational potential for the H_2 is higher than 2-fold or that the rotational motion is coupled. The rotational energy levels of a dumbbell molecule in an octahedral field, for example, are such that the ground state is composed of three[26] sublevels. Two of the three possible transitions within this ground state would be observable by INS, which could then give rise to a resolved doublet. Careful consideration of available crystal structure information,[6,8,14] as well as the results of the theoretical calculations discussed below, shows that the simple double-minimum potential used[5] in our analysis is clearly the appropriate model for the orientational potential of the H_2 and that therefore the observed structure in the rotational tunneling spectra cannot arise from the presence of additional potential minima. Finally, studies on methyl group tunneling[27] have in some cases shown splitting of the rotational tunneling peaks as a result of coupling between neighboring methyl groups. Such an effect is highly unlikely in the present case because the H_2 groups are too widely separated and may not interact in this way with the phosphine ligands since the latter have much smaller rotational constants and therefore much slower motions.

Theoretical Results

Geometrical Structures. The primary focus of the theoretical calculations is on the H_2 ligand rotational barrier. Before this issue is examined, however, the geometrical structures of these complexes will be discussed in order to assess the reliability of predicting M–H_2 geometries, since the rotational barrier depends sensitively on the M–H_2 distance. This becomes especially important in the case of Mo–H_2 complexes where to date there exist no reliable experimental data from neutron or X-ray diffraction studies about the geometrical parameters of the H_2 ligand. In contrast, the H_2 geometrical parameters have been refined for $W(CO)_3(P\text{-}i\text{-}Pr_3)_2(H_2)$.

In Table II the predicted structures from SCF calculations on model $M(CO)_3(PH_3)_2(\eta^2\text{-}H_2)$ complexes for M = W and Mo are compared. As noted earlier, the geometry of the $M(CO)_3(PH_3)_2$ fragment was held fixed in accord with the experimental X-ray diffraction information. The M–H_2 and H–H distances were then optimized subject to this constraint. Although metal–ligand distances can typically be overestimated by 0.1–0.2 Å in calculations of this type, the calculated W–H bond distance (1.91 Å) and H–H separation (0.812 Å) are in close agreement with the values from the neutron diffraction study (1.89 and 0.82 Å, respectively). The agreement may be compared to a previous calculation by Hay[3d] where a much longer W–H bond length (2.615 Å) was found. These calculations differ only in the treatment of the inner 5s and 5p electrons; in the earlier calculation these inner electrons were treated as core with an RECP, while in the present calculation these electrons were treated explicitly (like the 5d, 6s, and 6p valence orbitals). The 5s and 5p electrons have a spatial extent similar to the 5d electrons that are primarily responsible for the binding of H_2 to the metal. Apparently for cases where the metal–ligand interaction potential is quite flat, the predicted geometries can be sensitive to the quality of the description of the outer orbitals on the metal. Motion of the H_2

(26) Smith, D. *J. Chem. Phys.* **1978**, *68*, 3222.
(27) Heidemann, A. *Springer Proc. Phys.* **1987**, *17*, 44.

Chart II

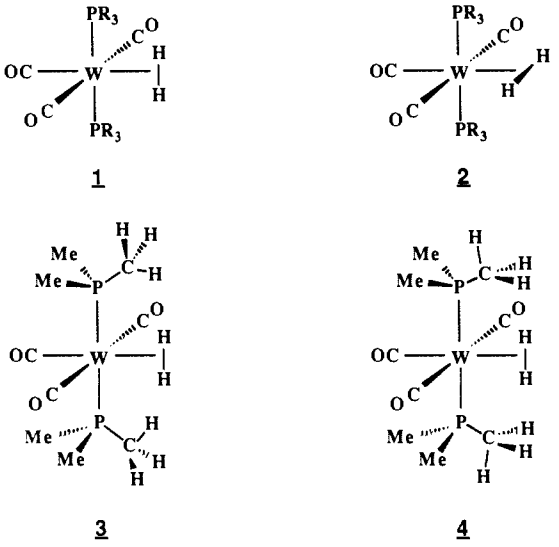

Table III. Calculated Rotational Barriers[a] for $M(CO)_3(PR_3)_2(H_2)$ Complexes from ab Initio Calculations

M	R	basis set: PR_3	basis set: CO	rotational barrier (kcal/mol)	H_2 binding energy (kcal/mol)
W	H	MBS	MBS	1.6	20
		DZ	MBS	1.4	19
		DZ	DZ	1.8	15
W	Me	MBS	MBS	0.8	20
Mo	H	DZ	MBS	0.0	14
		DZ	DZ	0.6	10

[a] Barriers were calculated for the following geometries (see text): $r(W-H_2)$ = 1.845 Å, $r(H-H)$ = 0.82 Å; $r(Mo-H_2)$ = 1.95 Å, $r(H-H)$ = 0.78 Å.

ligand over a 0.3-Å range about the minimum M–H separation, for example, results in changes in energy of only 2.5 kcal/mol.

The predicted Mo–H separation (1.99 Å) and H–H separation (0.78 Å) are consistent with a weaker M–H interaction and a less highly activated H_2 ligand in that the M–H distance is longer and the H–H distance is shorter for Mo than for W. The Mo complex is known to bind H_2 less strongly on the basis of IR data (see below) and its instability toward partial H_2 dissociation in solution [25 °C (1 atm of H_2)].[1] Although there are no experimental structural data with which to compare, one would expect that these calculated distances would be accurate within a few hundredths of an angstrom on the basis of the W calculations above.

The vibrational frequencies of the two symmetric (a_1) modes associated with M–H and H–H stretches are also given in Table II. These values are obtained assuming no coupling with the rest of the molecule and represent harmonic values. The predicted H–H frequencies decrease as one proceeds from uncomplexed H_2 (4523 cm^{-1}) to Mo–H_2 (3834 cm^{-1}) to W–H_2 (3181 cm^{-1}) in accord with the observed experimental trend. In both the calculated and experimental data, the M–H_2 stretch increases going from Mo to W.

Calculated Rotational Barrier. The barrier to rotation of the H_2 about the M–H_2 axis was obtained by a direct calculation of the difference in total energies between the two structures with the H_2 aligned along the P–M–P axis (**1**) and with the H_2 aligned along the OC–M–CO axis (**2**) (Chart II). As the H_2 was rotated, the other geometrical parameters were held fixed. The results for W and Mo complexes of H_2 with PH_3 and PMe_3 ligands are shown in Table III for various basis sets.

The calculated rotational barrier for the $W(CO)_3(PH_3)_2(H_2)$ complex is found to be 1.4–1.8 kcal/mol depending on the size of the basis set used for the ligands. This result is the same when one uses either the experimental or the predicted W–H and H–H distances, since there was little difference between these geometrical values. These rotational barriers contrast with the barrier of only 0.3 kcal/mol obtained by the use of the much longer W–H_2 bond length (2.1 Å) predicted from the earlier calculation.[3d] Since the rotational barrier decreases rapidly as the M–H bond length increases (Figure 5), it is essential that realistic bond lengths be used when calculating these barriers.

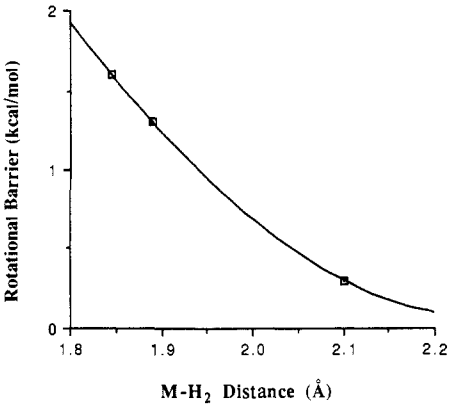

Figure 5. Calculated ab initio rotational barrier for $W(CO)_3(PH_3)_2(H_2)$ as a function of M–H_2 (centroid) distance with the use of the MBS description of the ligands.

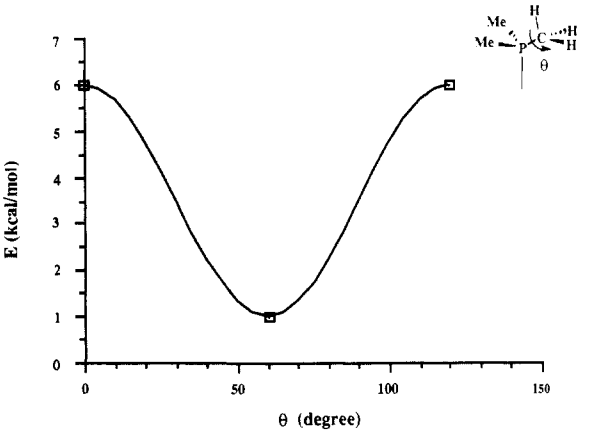

Figure 6. Barrier for rotation of Me groups about the P–C axis with eclipsed form, θ = 0°, and staggered form, θ = 60°.

With a more realistic PMe_3 ligand in the smaller basis (MBS), the calculated rotational barrier is somewhat smaller (0.8 kcal/mol) than in the equivalent calculation for the PH_3 ligand (1.6 kcal/mol). The binding energies of the H_2 ligand for both phosphine complexes were comparable: 20 kcal/mol (MBS). These calculated barriers may be compared to the experimentally observed values of 2.2–2.4 kcal/mol for phosphine ligands with R = *i*-Pr and Cy. Further comparisons of theoretical and experimental values are given in the Discussion.

For the Mo complex, a smaller calculated rotational barrier (0.6 kcal/mol) is consistent with the longer calculated M–H distance (1.99 Å for Mo versus 1.91 Å for W). Although there is no current experimental information on Mo–H_2 bond distances from diffraction studies, the close agreement between the calculated and observed distances in the W case (Table II) suggests that the above bond length for Mo should be quite reasonable. These results are also consistent with the rotational barriers of 1.5–1.7 kcal/mol for the H_2 complex of Mo with R = Cy, which is nearly 1 kcal/mol lower than that for the analogous W complex.

Another issue concerns the orientational influence of the phosphine ligands on M–H_2 rotational barriers. For the case of model ligands such as PH_3 such questions do not arise, but for PMe_3 we have found that the orientation of the ligand does affect the motion of the H_2, but only to a small degree. Before considering ligand–H_2 interactions, let us first examine an isolated PMe_3 ligand. For rotation of the CH_3 groups about the P–C bonds, there is a barrier of 5 kcal/mol for a synchronized motion of all three CH_3 groups about their respective axes (Figure 6), with the eclipsed (θ = 0°) form highest in energy and the staggered (θ = 60°) lowest. The combination of the intramolecular rotational

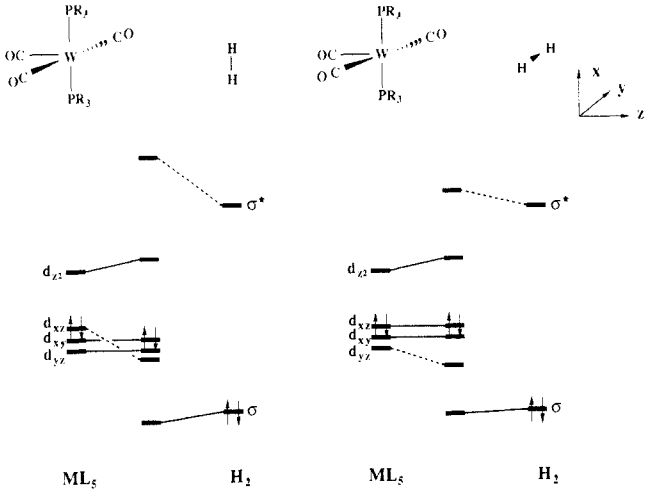

Figure 7. Orbital interaction diagram for ML_5 fragment and H_2 fragment with the H_2 fragment oriented at 0° and 90° to the P–M–P axis.

barrier in the PMe_3 ligands (10 kcal/mol for both phosphines) with additional unfavorable steric interactions in the molecule results in structure **3** being less stable by 15 kcal/mol overall than **4**, where in each case the H_2 ligand is aligned parallel to the P–M–P axis (Chart II). These interactions have surprisingly little effect on the actual rotational barrier of the H_2 itself. For the preferred orientation of the PMe_3 groups in **4**, the calculated barrier is 0.8 kcal/mol—somewhat smaller than the 1.6 kcal/mol result from the equivalent calculation with PH_3 groups. By comparison, for the unfavorable orientation of the PMe_3 groups in **3**, there is essentially no barrier (less than 0.1 kcal/mol). These results, namely *smaller* H_2 rotational barrier as the apparent phosphine R-group "contact" with H_2 *increases* on going from PH_3 complex to **4** to **3**, are counterintuitive but actually parallel an equally unexpected "inverse" relationship found in molecular mechanics calculations detailed below.

Molecular Mechanics Calculations. In order to more directly evaluate steric interactions that could contribute to the rotational barrier for dihydrogen, MM2 calculations were carried out. The results show the presence of a small, essentially sinusoidal barrier, the result of the large sum over pairwise interactions where most of the atoms are located around either of the phosphorus atoms. In the case of the PCy_3 complexes where the H_2 ligand was not located crystallographically,[14] an H_2 was artificially placed at various M–H distances: 1.79, 1.89 (the crystallographic distance for the W–P-*i*-Pr_3 complex), and 1.99 Å. The calculated barrier varied only slightly (0.9, 0.6, and 0.6 kcal/mol, respectively). Surprisingly, in all cases *the lower energy state corresponded to that for the H–H bond parallel to the P–W–P axis*, as found in the crystal structure of $W(CO)_3(P\text{-}i\text{-}Pr_3)_2(H_2)$. This orientation had been anticipated to be the higher energy state because steric repulsion by the bulky phosphine alkyl groups at first glance would have appeared to be the dominant factor. Further unexpected was the *higher* barrier for the complex with the less bulky P-*i*-Pr_3 ligand (1.4 kcal/mol) and the even higher barrier (2.0 kcal/mol) for an artificial species with alkyl groups completely clipped off the phosphorus atom (i.e., sterically similar to a PH_3 complex). These results must then be interpreted to mean that *the carbonyls cis to the H_2 exert more repulsion than the phosphines* (an alternative explanation based on an attractive potential between the P atoms and H_2 could not be substantiated upon close examination of the potentials). This is reasonable in that the CO ligands and the H_2 protons are bound more tightly to the metal than are the phosphines and, consequently, would be closer to each other when eclipsed than would eclipsed H_2 and phosphorus. Thus, the seemingly paradoxical decreases in the rotational barrier upon the increase of the size of the alkyl substituents on phosphorus can be explained as a relative destabilization of the lower energy state (H_2 oriented toward phosphorus) as compared to the higher energy state (H_2 aligned along OC–M–CO). The main conclusion drawn from the calculations is that neither the bulkiness of the phosphines nor the other steric factors significantly hinder H_2 rotation in these complexes.

Table IV. Energies ($-e_i$) of Highest Occupied Orbitals

R	ab initio (eV) MBS	ab initio (eV) DZ	Fenske–Hall (eV)
	PR_3 Ligands		
H	10.2	10.1	12.4
Me	7.6	8.4	9.3
i-Pr			9.1
Cy			8.8
	$W(CO)_3(PR_3)_2$ Fragment		
H	5.8	7.3	5.4
Me	4.8		4.8
i-Pr			4.3
Cy			4.1
	$Mo(CO)_3(PR_3)_2$ Fragment		
H	6.3	7.6	5.9
Me			4.9
Cy			4.5

Table V. Comparison of Metal d-Orbital Splitting Energies and H_2 Rotational Barriers in $M(CO)_3(PR_3)_2(H_2)$ Complexes from ab Initio Calculations

M	R	basis set PR_3	basis set CO	$e(d_{xz}) - e(d_{yz})$ (eV)	calcd rotational barrier (kcal/mol)
W	H	MBS	MBS	0.07	1.6
		DZ	MBS	0.08	1.4
		DZ	DZ	0.36	1.8
W	Me	MBS	MBS	−0.04	0.8
Mo	H	DZ	DZ	0.18	0.6

Orbital Interactions. The nature of the rotational barriers in these complexes ultimately arises from the orbital interactions between the metal $M(CO)_3(PR_3)_2$ fragment and the H_2 molecule. In this section the nature of these interactions is examined on the basis of the orbitals from the ab initio calculations and from Fenske–Hall calculations.

The key interactions arise from the following orbitals (see Figure 7): the set of three filled orbitals having predominantly d_{xy}, d_{xz}, and d_{yz} character with a_2, b_1, and b_2 symmetry designations, respectively; the filled σ-bonding orbital (a_1) and the empty σ^*-antibonding orbital of H_2; and the empty (denoted as d_{z^2} in Figure 7) d–s–p hybrid orbital of the metal fragment oriented toward the vacant sixth coordination site. When the H_2 is oriented in the *xz* plane, its σ^* has b_1 symmetry and can interact with d_{xz}, whereas when H_2 is oriented in the *yz* plane, it has b_2 symmetry and can interact with d_{yz}. The filled H_2 σ orbital can donate electron density into the vacant metal d_{z^2} orbital in forming the $M–H_2$ bond, but there is no orientational preference for this process. Because the CO ligands can stabilize the d orbitals more effectively by back-bonding into the π^* orbitals, the overall ordering of the d levels generally results: $d_{yz} < d_{xy} < d_{xz}$. With the d_{xz} orbital lying highest in energy, the interaction with the H_2 σ^* favors the orientation where the H_2 lies in the *xz* plane aligned with the P–M–P axis as observed experimentally and as obtained from the ab initio calculations. From this argument, one would expect a correlation between the difference in energies, $e(d_{xz}) - e(d_{yz})$, and the rotational barrier since these are the only orbitals in the above set with the anisotropic interactions with H_2 through the σ^* orbital. As shown in Table IV, however, the differences in orbital energies of the $M(CO)_3(PR_3)_2$ fragment in the ab initio calculations are rather small and do not show a particularly strong correlation with the computed barriers. However, for the best calculations (DZ on all ligands) the orbital splittings are 0.36 and 0.18 eV for the W and Mo fragments, respectively, and the rotational barriers also follow this trend, 1.8 and 0.6 kcal/mol for W and Mo.

Before turning to analysis of Fenske–Hall results, the effects of varying the basicity of the phosphine groups are shown in Table V where the energies of the highest occupied orbital in the PR_3 ligand and in the corresponding metal complex are shown from

Table VI. Analysis of H_2 Rotational Barriers from Fenske–Hall Calculations on $M(CO)_3(PR_3)_2(H_2)$ Complexes

M	R	fragment $e(d_{xz}) - e(d_{yz})$ (eV)	H_2 complex changes in d orbitals (90°–0°) calcd (kcal/mol)	H_2 complex changes in d orbitals (90°–0°) normalized[a] (kcal/mol)
W	H	1.38	0.94	1.89
	Me	1.56	−0.76	1.61
	i-Pr	1.71	−0.22	1.78
	Cy	1.70	0.00	1.48
Mo	H	1.30		0.94
	Me	1.55		0.95
	Cy	1.67		0.97

[a] See text for definition of "normalized".

both ab initio and Fenske–Hall results. The same overall trends are found for the two types of calculations. First, as the H is replaced by progressively bulkier alkyl groups, the highest orbital becomes higher in energy and, hence, a better potential electron donor. This increased donor potential, in turn, is reflected in the increase in energy of the highest occupied d orbital in the complex, which would occur as more electron density is shifted to the metal.

In the Fenske–Hall calculations, since one cannot compute directly a barrier to rotation by comparing the differences in energies of the two structural forms, two alternative approaches have been pursued in order to understand the electronic effects of the bulkiest phosphine ligands. In the first methods, the differences in the sum of the orbital energies of the three highest (predominantly d-like) orbitals were simply compared for the two orientations, **1** and **2**, of the H_2 ligand (Chart II; $\theta = 0°$ and $\theta = 90°$). As shown in Table VI, this technique does not lead to consistent trends for the various ligands.

In the second method, from the sum of orbital energies for a particular orientation was subtracted the corresponding sum of diagonal elements of the ML_5 fragment, and this "normalized" sum was then compared for the two structures. This approach, in each case, predicted the correct orientation and led to similar "barriers" for the alkylphosphine ligands that were slightly higher than those for the PH_3 ligands. The "normalization" is justified in that the method does not fix the diagonal elements, but rather calculates them in each case. This determination limits the direct comparison of results for different orientations, and thus, the normalization procedure was employed.

Finally we note that all of the theoretical calculations have used experimentally determined geometries for the $M(CO)_3(PR_3)_2$ framework in order to model as closely as possible the molecular environment of the H_2 as probed in the neutron scattering experiments reported here. The other alternative would have been to use fully optimized theoretical structures in which all geometrical degrees of freedom in the molecule are relaxed for each orientation of the H_2. However, the experience to date on other complexes suggests that the metal–ligand distances, for example, would be overestimated by 0.1–0.2 Å from such Hartree–Fock calculations, raising the question of whether the geometries and rotational barriers of the H_2 adducts would be well treated.

Discussion

Metal–dihydrogen complexes, especially those that also contain classical hydride ligands, exhibit a wide range of dynamic behavior, including reversible H_2 dissociation, tautomeric equilibrium between dihydrogen and dihydride forms, fluxionality, dihydrogen–hydride exchange, and H_2 reorientation, specifically rapid rotation in one plane. This paper has focused upon the latter motion, which, in addition to providing direct information on metal–H_2 bonding, also is of important consequence in NMR techniques used to estimate H–H distances from T_1 data[28] and in broadening effects on H–H infrared stretching frequencies.[1,29]

Table VII. Observed and Calculated Barriers to η^2-H_2 Rotation (kcal/mol)

		observed barrier	calculated barrier: steric	calculated barrier: electronic	
M	R	INS	MM2[a]	ab initio[b]	Fenske–Hall[a]
W	Cy	2.2[c]	0.6	1.8[d] (0.8[e])	1.5
W	*i*-Pr	2.4[c]	1.4	1.8[d] (0.8[e])	1.8
Mo	Cy	1.5[f] (1.7[c])	0.6	0.6[d]	1.0

[a] r(H–H) = 0.82 Å and r(W–H) = 1.89 Å; r(H–H) = 0.82 Å and r(Mo–H) = 1.99 Å. [b] r(H–H) = 0.82 Å and r(W–H) = 1.89 Å; r(H–H) = 0.78 Å and r(Mo–H) = 1.99 Å. [c] r(H–H) = 0.82 Å. [d] For R = H. [e] For R = Me. [f] r(H–H) = 0.79 Å.

The barriers to H_2 rotation were readily obtained by inelastic neutron scattering techniques, wherein the observation of rotational tunneling modes even at relatively high temperatures (near 200 K) also points to the significance of *quantum mechanical effects in hydrogen coordination to transition metals*. The recent observation of exchange couplings in the solution NMR of certain polyhydride complexes reinforces this notion.[30]

It would appear from our results that the barrier to H_2 rotation in $M(CO)_3(PR_3)_2(H_2)$ is determined to a large extent by the direct H_2–metal interaction and to a somewhat smaller extent by steric effects from the phosphine ligands. The improved ab initio calculations and the Fenske–Hall calculations were used as a measure of the portion of the barrier resulting from the electronic interaction between H_2 and the metal, while the MM2 calculations on these systems addressed the magnitude of the steric effects. The latter showed no large direct steric effects of the bulky phosphine ligands on the H_2 rotational barriers but rather showed a small unanticipated orientational preference for the H_2 parallel to the P–M–P axis. The results for these calculations are summarized in Table VII and compared with the experimental values derived from the INS data. It must be emphasized at this point that all of the calculational methods find the same simple double-minimum potential with the minima along the P–M–P axis, wich is indeed observed to be the equilibrium position for the H_2 in the crystallographic studies. If one assumes that the MM2 method treats only the steric effects, i.e., nonbonded interactions between η^2-H_2 and the other atoms of the complex as a function of H_2 rotation angle, and that the ab initio theory accounts primarily for the direct electronic interaction between the H_2 and the metal, one may add barrier heights from the two calculations to arrive at an effective total barrier. These assumptions are not unreasonable in that replacement of W with Mo, which changes the electronic environment, has no noticeable effect on the value of the barrier calculated from MM2 while the barrier derived from electronic structure calculations does not change greatly with phosphine size (PH_3 versus PCy_3). The results of the calculations are compared with the experimentally derived values in Table VII for the three complexes of the present study. It may be noted that the agreement is qualitatively rather good. For example, ab initio theory correctly gives a larger barrier in the case of the W complex than that in the Mo analogue, while the MM2 result for the P-*i*-Pr_3 ligand is greater than that for PCy_3. In both cases, however, the differences are larger than what is actually observed from INS.

As far as the relative importance of the two contributions to the experimentally observed barrier to rotation is concerned, the somewhat larger uncertainties inherent in the calculations make it difficult to reach a definitive conclusion. While the relatively large change (0.8 kcal/mol) calculated by MM2 when PCy_3 is replaced with P-*i*-Pr_3 on the W complex is not quantitatively consistent with the experimental observation (0.2 kcal/mol), it is nevertheless the case that for the W–PCy_3 complex the sum

(28) (a) Bautista, M. T.; Earl, K. A.; Maltby, P. A.; Morris, R. H.; Schweitzer, C. T.; Sella, A. *J. Am. Chem. Soc.* **1988**, *110*, 7031. (b) Hamilton, D. G.; Crabtree, R. H. *Ibid.* **1988**, *110*, 4126.

(29) (a) Upmacis, R. K.; Poliakoff, M.; Turner, J. J. *J. Am. Chem. Soc.* **1986**, *108*, 3645. (b) Gadd, G. E.; Upmacis, R. K.; Poliakoff, M.; Turner, J. J. *Ibid.* **1986**, *108*, 2547. (c) Sweany, R. L.; Moroz, A. *Ibid.* **1989**, *111*, 3577.

(30) Zilm, K. W.; Heinekey, D. M.; Millar, J. M.; Payne, N. G.; Demou, P. *J. Am. Chem. Soc.* **1989**, *111*, 3088.

of the barriers, MM2 (0.6 kcal/mol) + ab initio calculated steric and electronic or Fenske–Hall (1.8 or 1.5 kcal/mol), agree, perhaps fortuitously, with experiment (2.2 kcal/mol). The lack of precise crystallographic information on the H_2 location in the PCy_3 compounds does of course lead to some inherent inaccuracy in the comparison to the P-*i*-Pr_3 analogue. For example, the MM2 barrier for the PCy_3 compounds changes from 0.6 kcal/mol for a M–H distance of 1.89 Å (observed in W–P-*i*-Pr_3) to 0.9 kcal/mol for a separation of 1.79 Å, although increasing the distance to 1.99 Å (estimated for the Mo species from ab initio results) gives no change. There is also a small uncertainty in the barrier determined by INS for $Mo(CO)_3(PCy_3)_2(H_2)$ (Table VII) because it depends on the value of the reduced rotational constant B, which in turn depends on the H–H distance. Setting H–H to 0.82 Å, the experimental value for the W–P-*i*-Pr_3 complex, gives 1.7 kcal/mol while employing the 0.79 Å estimate from ab initio calculation gives 1.5 kcal/mol. The latter distance is probably more reasonable because of the known weaker binding of H_2 to Mo than W. Presumably the H–H separation in the W–PCy_3 complex is similar to that in the W–P-*i*-Pr_3 complex.

In summary, it must be noted that the agreement between the calculated and observed barriers to H_2 rotation is remarkably good, particularly in view of the small barrier heights involved and the limitations imposed by the lack of certain structural information. A meaningful detailed analysis of a dynamic process involving such low energies could not have been predicted. Most importantly, the data reveal that the direct electronic binding of the dihydrogen contributes significantly to this barrier, i.e., about half or more of the experimentally determined value. The rotational tunnel splitting is an extremely sensitive measure of this barrier as it depends exponentially[4b] on the value of the barrier. Thus, for example, the observation of a higher barrier (760 vs ~500 cm^{-1}, i.e., stronger M–H_2 binding) in the W complex compared with the Mo analogue is in agreement with a higher M–H_2 infrared stretch (ν_s = 953 cm^{-1} (M = W) versus 871 cm^{-1} (M = Mo)), but the effect on the rotational tunnel splitting is much more pronounced. It is therefore clear that rotational tunneling spectroscopy of η^2-bound H_2 by inelastic neutron scattering can be used as a probe of the electronic details of M–H_2 binding, since the directional properties of the electron wave functions, which help optimize the electron flow ($H_2 \rightarrow M$ σ donation, $M \rightarrow H_2$ σ^* back-donation) between H_2 and metal, also seem to be largely responsible for the barrier to rotation of the dihydrogen. Experimental evidence for metal to dihydrogen σ^* back-bonding is thus attainable as long as steric influences are minimal. The observation of rotational tunneling modes can also be expected to be an unambiguous diagnostic for H_2 binding, especially in complexes for which NMR or crystallographic evidence is tenuous.

Further INS experiments involving solution-state studies and dihydrogen complexes with different ligands and metals have been initiated to gain a more complete picture of the relationship of the rotational barrier to the bonding and ligand dynamics of these systems. Rotational tunneling peaks have been located by INS for iron complexes containing both H_2 and hydride ligands studied by other groups, and rotational barriers have been determined.[31] It is anticipated from preliminary experiments that quasi-elastic neutron-scattering studies will be useful in studying dynamic processes such as intramolecular exchange between H_2 and hydride ligands in these and other complexes containing both types of ligands.

Acknowledgment. We thank H. Blank of the Institut Laue-Langevin for assistance with some of the experiments; Robert R. Ryan for suggestions concerning MM2 and other aspects of the problem; and David Clark for aid with graphics programs. Work at Los Alamos was performed under the auspices of the U.S. Department of Energy, Division of Chemical Sciences, Office of Basic Energy Sciences. The work has also benefited from the use of facilities at the Los Alamos Neutron Scattering Center, a national user facility funded as such by the Department of Energy, Office of Basic Energy Sciences.

(31) (a) Eckert, J.; Blank, H.; Bautista, M. T.; Morris, R. H. *Inorg. Chem.*, in press. (b) Van Der Sluys, L. S.; Eckert, J.; Eisenstein, O.; Hall, J. H.; Huffman, J. C.; Jackson, S. A.; Koetzle, T. F.; Kubas, G. J.; Vergamini, P. J.; Caulton, K. G. *J. Am. Chem. Soc.*, in press.

Copper-Mediated Oxidative C-Terminal N-Dealkylation of Peptide-Derived Ligands. A Possible Model for Enzymatic Generation of Desglycine Peptide Amides

K. Veera Reddy, Shiow-Jen Jin, Pramod K. Arora, David S. Sfeir, S. C. Feke Maloney, F. L. Urbach, and Lawrence M. Sayre*

Contribution from the Department of Chemistry, Case Western Reserve University, Cleveland, Ohio 44106. *Received August 21, 1989*

Abstract: A number of Cu(II) complexes of peptide derivatives that coordinate via N-deprotonation at the C-terminal amino acid residue have been characterized by titrimetry and the Cu(III)–Cu(II) electrochemical potentials. Reaction of these complexes with persulfate induces oxidative decarboxylation and hydrolysis of the resulting *N*-acylimines to carboxamide and either HCHO, CH_3CHO, or acetone depending on the identity of the C-terminal residue (Gly, Ala, or Aib, respectively). For complexes with Cu(III)–Cu(II) potentials of +1.4 V vs NHE or lower, reaction with $IrCl_6^{2-}$ results in C–N dehydrogenation at the C-terminus, giving (after hydrolysis) carboxamide and either glyoxylic or pyruvic acid for C-terminal Gly or Ala. In the case of C-terminal Aib, Ir(IV) oxidation results in a very slow production of acetone. Complexes with E_p above +1.5 V do not react with $IrCl_6^{2-}$, and sarcosine-terminal complexes, as well as those containing phenolate ligation, are inert to both persulfate and Ir(IV). The optimal complex studied here for investigating the mechanism of C–N dehydrogenation was picolinyl–Aib–Ala (E_p = +0.882 vs NHE), in which case the Ir(IV)-mediated cleavage to pyruvic acid and picolinyl–Aib–NH_2 proceeds via a Cu(III) intermediate. The same transformation could be effected electrochemically. The C-terminal oxidative N-dealkylation reaction, induced by Cu(III), has not been previously observed and may be a relevant model for the copper enzyme peptidyl α-amidating monooxygenase, which is responsible for conversion of glycine-extended peptide prohormones to the biologically active peptide carboxamides.

The majority of physiologic secretory polypeptide hormones, as well as many neuropeptides in the central nervous system, are COOH-terminal *amides*,[1] examples being gastrin, choleocystokinin, α-MSH, calcitonin, vasopressin, secretin, and certain

0002-7863/90/1512-2332$02.50/0